Original article [1]

Saponin-rich fractions from quinoa scarification residues (*Chenopodium quinoa* Willd): Chemical characterization and evaluation of antioxidant and anti-inflammatory activities

Carolina Triguero[1], Maribel Lozano[1] , Yonny R. Flores[1], Eduardo Gonzales[2], Silvia Zambrana[2] and Giovanna R. Almanza[1,*]

[1]Instituto de Investigaciones Químicas IIQ-*Bioorgánica* Universidad Mayor de San Andrés, La Paz; [2]Instituto de Investigaciones Fármaco-Bioquímicas IIFB-*Farmacología*, Universidad Mayor de San Andrés, La Paz

Keys: *Quinoa residues, Mojuelo, Saponin-rich fractions, LC–MS profiles, Phenolic compounds, In vitro, anti-inflammatory, antioxidant;* **Claves:** *Residuos De Quinua, Mojuelo, Fracciones Ricas En Saponinas, Perfiles LC-MS, Compuestos Fenólicos, In Vitro, Antiinflamatorio, Antioxidante.*

ABSTRACT

Quinoa processing residues, including mojuelo, are promising sources of bioactive compounds. This study designed a fractionation strategy to obtain saponin-enriched extracts through liquid–liquid partitioning and chromatographic separation, followed by LC–ESI–MS in positive ion mode. The hydroalcoholic extract contained 49.6% saponins and 19.7% phenolics. Mass spectrometry identified oleanane-type saponins and phenolic compounds. A major bidesmosidic saponin [3-O-β-D-glucopyranosyl-(1→3)-α-L-arabinopyranosyl -phytolaccagenic acid 28-O-β-D-glucopyranosyl] and the flavonoid mauritianin were isolated and used as standards. Fractionation raised saponin purity above 94%, while phenolics remained in crude extracts, which showed the strongest antioxidant activity in ABTS and DPPH assays. In vitro tests with LPS-stimulated RAW 264.7 macrophages revealed that saponin-rich fractions suppressed nitric oxide, TNF-α, and IL-6, and reduced PGE_2 and LTC_4, suggesting modulation of COX-2 and 5-LOX pathways. These findings support quinoa residues as valuable nutraceutical resources.

RESUMEN

Residuos de quinua ricos en saponinas: Caracterización y evaluación antioxidante/antiinflamatoria. Los residuos del procesamiento de quinua, incluido el mojuelo, constituyen una fuente prometedora de compuestos bioactivos. Este estudio diseñó una estrategia de fraccionamiento para obtener extractos enriquecidos en saponinas mediante partición líquido–líquido y técnicas cromatográficas, seguida de análisis LC–ESI–MS en modo de ion positivo. El extracto hidroalcohólico presentó 49,6% de saponinas y 19,7% de compuestos fenólicos. La espectrometría de masas identificó saponinas tipo oleanano y diversos fenoles. Se aislaron un saponósido bidesmosídico [3-O-β-D-glucopiranosil-(1→3)-α-L-arabinopiranosil-á cido fitolaccagénico 28-O-β-D-glucopiranosil] y el flavonoide triglucosilado mauritianina, empleados como estándares. El fraccionamiento elevó la pureza de saponinas por encima del 94%, mientras los fenoles permanecieron en extractos crudos, que mostraron mayor actividad antioxidante en ensayos ABTS y DPPH. En pruebas in vitro con macrófagos RAW 264.7 estimulados con LPS, las fracciones ricas en saponinas redujeron óxido nítrico, TNF-α, IL-6, PGE_2 y LTC_4, sugiriendo modulación de las vías COX-2 y 5-LOX. Estos hallazgos respaldan la valorización de residuos de quinua como recursos nutracéuticos.

Revista Boliviana de Química, 2026, 43, 142-160
ISSN 0250-5460, Rev. Bol. Quim. ***Paper edition***
ISSN 2078-3949, Rev. boliv. quim. ***e-edition***
***Jan-Jun;* 30 junio 2026**

https://doi.org/10.53287/pyii9560fa11e

[1]Received May 12, 2026, accepted June 11, 2026, published June 30, 2026. *Mail to: galmanza@fcpn.edu.bo

INTRODUCTION

There is growing interest among companies, governmental institutions, and researchers worldwide in the optimal use and management of industrial waste in order to mitigate the effects of climate change impact[1] [2]. In Bolivia, quinoa (*Chenopodium quinoa* Willd.) processing generates a by-product known as *mojuelo*, which is produced in large quantities during the scarification of quinoa seeds prior to consumption. Considering that Bolivia is one of the main exporters of quinoa, this residue remains largely underutilized and accumulates as industrial waste.
However, several studies have reported the chemical composition of quinoa *mojuelo*, revealing a high content of oleanane-type saponins and glycosylated phenolic compounds (flavonoids and phenolic acids) along with primary metabolites such as proteins, free sugars, and fatty acids[3]. In general, quinoa saponins remain a major focus of research due to their wide range of biological activities, including anti-inflammatory, cytotoxic, fungicidal, pesticidal, and molluscicidal properties[4]. Consequently, there is increasing interest in adding value to quinoa *mojuelo* due to its high content of triterpenoid saponins.

Currently, quinoa saponins are attracting attention across diverse fields, including medicinal chemistry, agriculture, food science, environmental applications, and the cosmetic industry[5] [6]. Chemically, quinoa saponins occur as complex mixtures of more than 90 different structures[7], which have been identified using a variety of chromatographic and spectroscopic techniques. This structural diversity makes their chromatographic separation challenging, while their relatively high molecular weight limits the applicability of conventional separation methods[8]. Although several procedures for saponin purification and isolation have been reported, there is still a lack of studies describing the combination of chromatographic methods to obtain quinoa fractions enriched in saponins suitable for further studies.

In this work, we propose a comprehensive procedure to obtain saponin-rich fractions from scarified quinoa residues *mojuelo* through the combination of complementary chromatographic approaches, including normal-phase (NP) and reverse-phase (RP) liquid chromatography. Chemical characterization was performed using LC-MS. This approach provides detailed information on enriched saponin fractions, which could be used as reference materials for more precise and accurate quantification of quinoa saponins. Furthermore, this methodology may facilitate the chromatographic separation and characterization of saponins from other natural sources, as well as the study of biological properties of quinoa saponins, like the anti-inflammatory and antioxidant activities of the enriched saponin fractions which were evaluated in this work.

RESULTS AND DISCUSSION

Chemical Characterization of the Hydroalcoholic Extract (HE)

Consistent with previous reports, the hydroalcoholic extract (**HE**) obtained from quinoa *mojuelo* contains a complex mixture of secondary metabolites, including oleanane-type saponins, glycosylated flavonoids, and glycosylated phenolic acids. In this work, these compounds were identified and confirmed using UV spectroscopy, TLC monitoring, and LC–ESI–MS analysis in positive ion mode (Figure 1). Furthermore, the **HE** contains primary metabolites such as proteins, quantified using the Kjeldahl method, and fatty acids characterized by GC–MS.

The inorganic fraction exhibited a complex mineral composition, mainly consisting of carbonates, silicates, halides, and metal oxides, as determined by X-ray diffraction (XRD). In view of this mineralogical complexity, complementary X-ray fluorescence (XRF) analysis was performed, confirming the presence of major elements (*Na, Mg, Al, Si, S, Cl, Ca*, and *Fe*) as well as trace elements (*Mn, Cu, Zn,* and *Rb*). The detection of *Si* and *Al* suggests the presence of aluminosilicate phases, whereas *Na, Mg*, and *Cl* are mainly associated with soluble salts, and *S* with sulfur-containing compounds. Furthermore, the relatively high intensities of *Ca* and *Fe* indicate the possible presence of carbonates, phosphates, and/or metal oxides. Overall, these findings highlight the physicochemical complexity of the extract and provide a robust analytical basis supporting its potential functional and biological applications.

HPLC and UV–Vis spectrophotometric analyses of the **HE** was used to determine the type of secondary metabolites in the chromatograms. Flavonoids exhibit characteristic absorption bands between 240–290 nm (associated with ring A) and 300–500 nm (associated with ring B conjugation). Phenolic acids typically show strong absorption in the 200–300 nm range, with a maximum around 280 nm. In contrast, triterpenoid saponins, such as oleanane-type compounds, display weak absorption between 200–250 nm due to the absence of strong chromophores. Figure 1 illustrates representative chemical structures and UV absorption patterns of the identified metabolite classes

Table 1. Chemical characterization of **HE** from quinoa *Mojuelo.*

Compounds in the HE	Identification Technique	Conc (%)	References
Saponins	TLC, foam, UV, LC–ESI–MS	49.6	[3]
Phenolic	TLC, UV, LC-MS	19.7	[9]
Inorganic	XRD, XRF	4.72	
Proteins	Kjeldahl	1.10	[10 11 12]
Fatty acids	GC–MS	1.12	[13]
Others	nd	23.8	

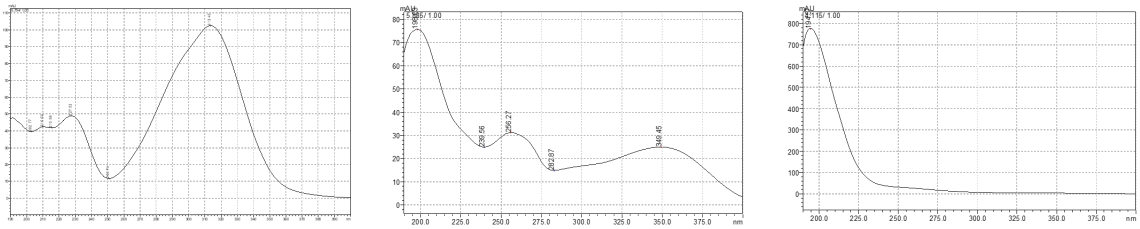

Phenolic acid Flavonoids Saponins

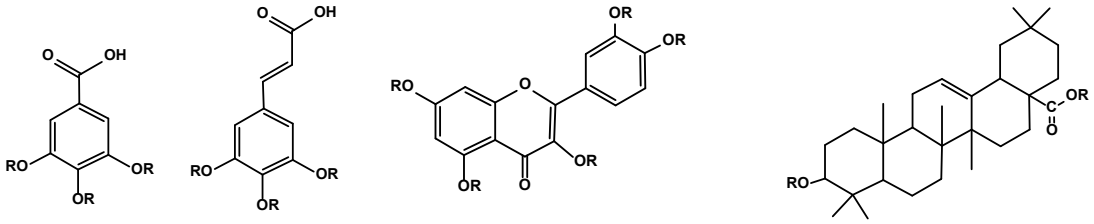

Figure 1. Typical chemical structures and UV absorption spectra of secondary metabolites of **HE**.

For the identification of saponins, phenolic compounds, and flavonoids in the **HE**, UV spectra and retention times obtained from HPLC chromatograms were considered. A total of 23 major peaks corresponding to secondary metabolites present in the extract were detected; however, some of these peaks may represent more than one compound. Compounds with short retention times (4.47–7.25 min) were assigned to glycosylated phenolic acids and flavonoids, characterized by absorption maxima between 260 and 350 nm. In contrast, peaks with retention times between 7.73 and 28.41 min were attributed to saponins, showing characteristic absorption at 210 nm. These peaks correspond to different aglycones, including phytolaccagenic acid (PA), hederagenin (HE), oleanolic acid[14], serjanic acid (SA) and a minor sapogenin just called sapogenin 5 (S5), which were determined by LC–ESI–MS in positive ion mode (Table 2).

Table 2 summarizes the peaks determined in the LC–ESI–MS chromatogram, including retention times, UV spectral data, and aglycone fragment ions obtained by LC–ESI–MS in positive ion mode. The chromatographic profile of **HE** shows peaks in the range of 4.09–28.41 min. Early-eluting signals (3.99–4.14 min) correspond to polar compounds and, in some cases, inorganic material, as suggested by XRD and XRF analyses, along with the absence of corresponding signals in NMR spectra. Peaks eluting between 4.47 and 7.25 min were tentatively assigned to glycosylated phenolic acids and flavonoids based on their UV absorption spectra and LC–ESI-MS fragmentation patterns, with enhanced detection at 350 nm. The identification of the aglycone moieties was achieved through comparison of MS fragmentation patterns with literature data. Peaks within the retention time range of 7.73–28.41 min were attributed to saponins, initially detected by RP-TLC and subsequently confirmed by their characteristic UV absorption at 210 nm. LC–ESI–MS analysis in positive ion mode revealed stable fragment ions corresponding to the aglycone moieties, and their structural assignment was further supported by comparison with previously reported data[7].

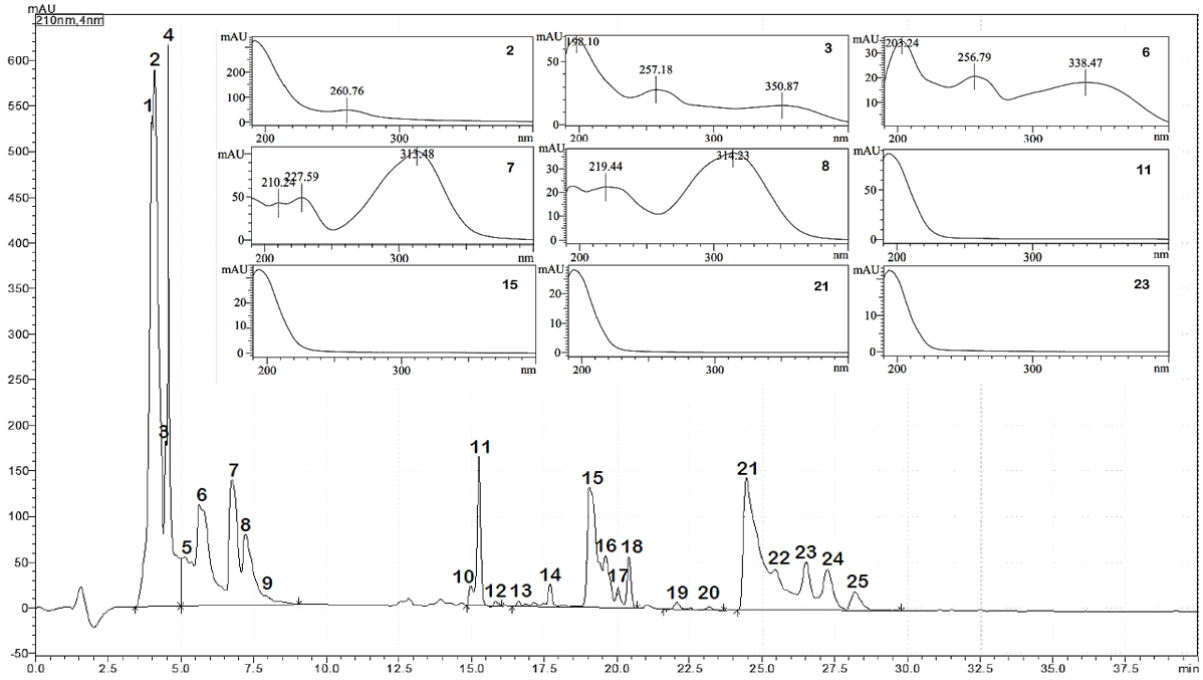

Figure 2. Peaks (1–25) detected in the HPLC–UV chromatogram of the hydroalcoholic extract (**HE**) at 210 nm, along with the UV spectra of peaks 2, 3, 6, 7, 8, 11, 15, 21, and 23.

Table 2. Peaks assigned in the LC–ESI–MS chromatogram of Hydroalcoholic Extract (**HE**) by analysis of MS and UV data.

Peak	T_R (min)	Assigned type of metabolite	UV λ max (nm)	Aglycone	Main MS fragments
1	3.99	nd	263.5	nd	nd
2	4.14	nd	260.7	nd	nd
3	4.47	Flavonoid	257.2- 350.8	Apigenin	274 $[M+H]^+$, 265, 193, 192, 163
4	4.56	Flavonoid	262.8-343.7	Luteolin	287 $[M+H]^+$, 273, 257, 221, 197, 181
5	5.12	Flavonoid	254.9-350.4	Quercetin	303 $[M+H]^+$, 294, 287, 235, 220, 205, 166
6	5.64	Flavonoid	257.8-338.5	Kaempferol	287 $[M+H]^+$, 165, 153, 137
7	6.78	Phenolic acid	227.6-313.5	CA	181 $[M+H]^+$, 163, 137
8	7.25	Phenolic acid	219.4-314.2	FA	195 $[M+H]^+$, 177, 149, 134
9	7.73	Saponin	220	S5	489 $[M+H]^+$, 471, 453, 435, 407
10	14.97	Saponin	220	PA	517 $[M+H]^+$, 499, 481, 471, 453, 247, 207
11	15.25	Saponin	220	PA	517 $[M+H]^+$, 499, 481, 471, 453, 247, 207
12	15.84	Saponin	220	PA	517 $[M+H]^+$, 499, 481, 471, 453 ,247, 207
13	16.61	Saponin	220	HE	473 $[M+H]^+$, 455, 437, 409, 391, 203
14	17.70	Saponin	220	PA	517 $[M+H]^+$, 499, 481, 471, 453, 247, 207
15	19.14	Saponin	220	HE	473 $[M+H]^+$, 455, 437, 409, 391, 203
16	19.71	Saponin	220	SA	501 $[M+H]^+$, 483, 455, 437, 293, 247, 191
17	20.13	Saponin	220	HE	473 $[M+H]^+$, 455, 437, 409, 391, 203
18	20.40	Saponin	220	HE	473 $[M+H]^+$, 455, 437, 409, 391, 203
19	22.05	Saponin	220	OA	457 $[M+H]^+$, 439, 441, 393, 249, 191
20	23.12	Saponin	220	OA	457 $[M+H]^+$, 439, 441, 393, 249, 191
21	24.67	Saponin	220	OA	457 $[M+H]^+$, 439, 441, 393, 249, 191
22	25.37	Saponin	220	OA	457 $[M+H]^+$, 439, 441, 393, 249, 191
23	26.45	Saponin	220	OA	457 $[M+H]^+$, 439, 441, 393, 249, 191
24	27.37	Saponin	220	OA	457 $[M+H]^+$, 439, 441, 393, 249, 191
25	28.41	Saponin	220	OA	457 $[M+H]^+$, 439, 441, 393, 249, 191

nd= non determined, CA= Caffeic acid, FA= Ferulic acid, PA= Phytolaccagenic acid, HE= Hederagenin, SA= Serjanic acid, AO = Oleanolic acid, S5 = Sapogenin 5.

Partition of HE between n-butanol (butanolic extract BE) and water (aqueous extract AE)

The **HE** was subjected to liquid–liquid partitioning with n-butanol, yielding an aqueous extract (**AE**) and a butanolic extract (**BE**). The chromatographic profile of the **BE** showed a marked enrichment in saponins and phenolic acids,

whereas the **AE** chromatogram predominantly displayed polar compounds and some more polar saponins (Figure 3). These differences confirm the effectiveness of liquid–liquid partitioning as a pre-enrichment strategy for saponins.

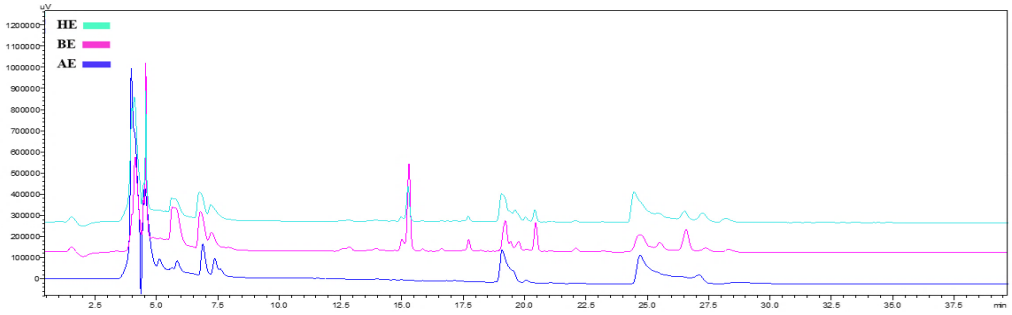

Figure 3. HPLC–UV chromatograms (210 nm) of the hydroalcoholic, aqueous, and butanolic extracts.

Procedures to obtain saponin-enriched fractions from BE and AE

Three different procedures were applied to obtain saponin-enriched fractions from **AE** and **BE**.

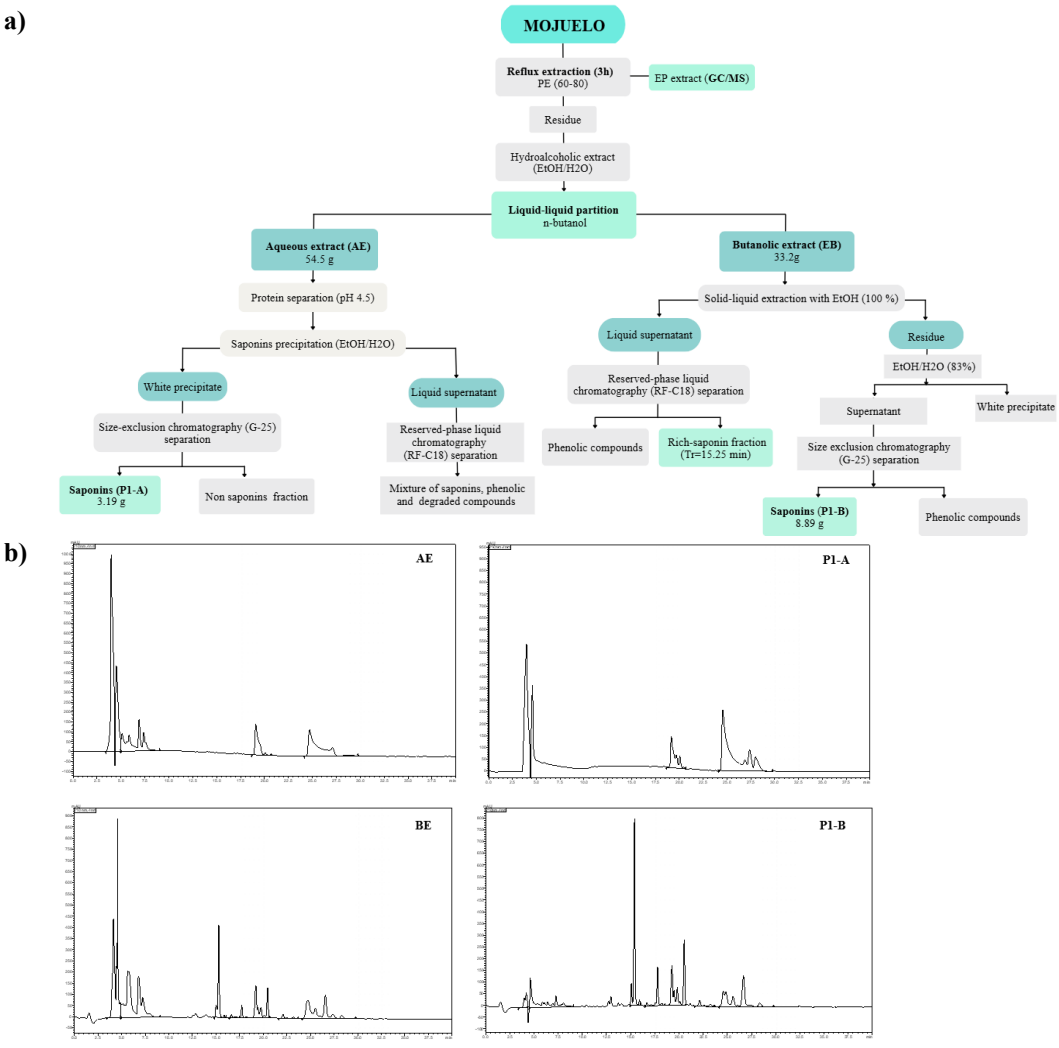

Figure 4. a) Scheme of obtention of saponin-enriched fractions **P1-A** from aqueous extract (**AE**) and **P1-B** from butanolic extract (**BE**), b) HPLC–UV chromatograms of **AE** and **BE** and their corresponding fractions **P1-A** and **P1-B**.

Procedure 1

AE and **BE** were subjected to Procedure 1 (Figure 4; see above and see Experimental Section for more details). Fractions **P1-A** (from **AE**) and **P1-B** (from **BE**) were selected due to their higher saponin content, as confirmed by LC–ESI–MS. As shown in Figure 4, **P1-B** exhibits a higher degree of purification in saponins, whereas **P1-A** still contains a significant proportion of phenolic compounds and other compounds.

Procedure 2

AE and **BE** were further subjected to reversed-phase C18 chromatography, yielding three fractions each. The first fraction did not contain saponins, while the second and third fractions contained mixtures of flavonoids, phenolic acids, and saponins in varying proportions. These fractions were further purified, resulting in two fractions (**P2-A** and **P2-B**) selected for subsequent analysis due to their high saponin content and reduced presence of other compounds (Figure 5).

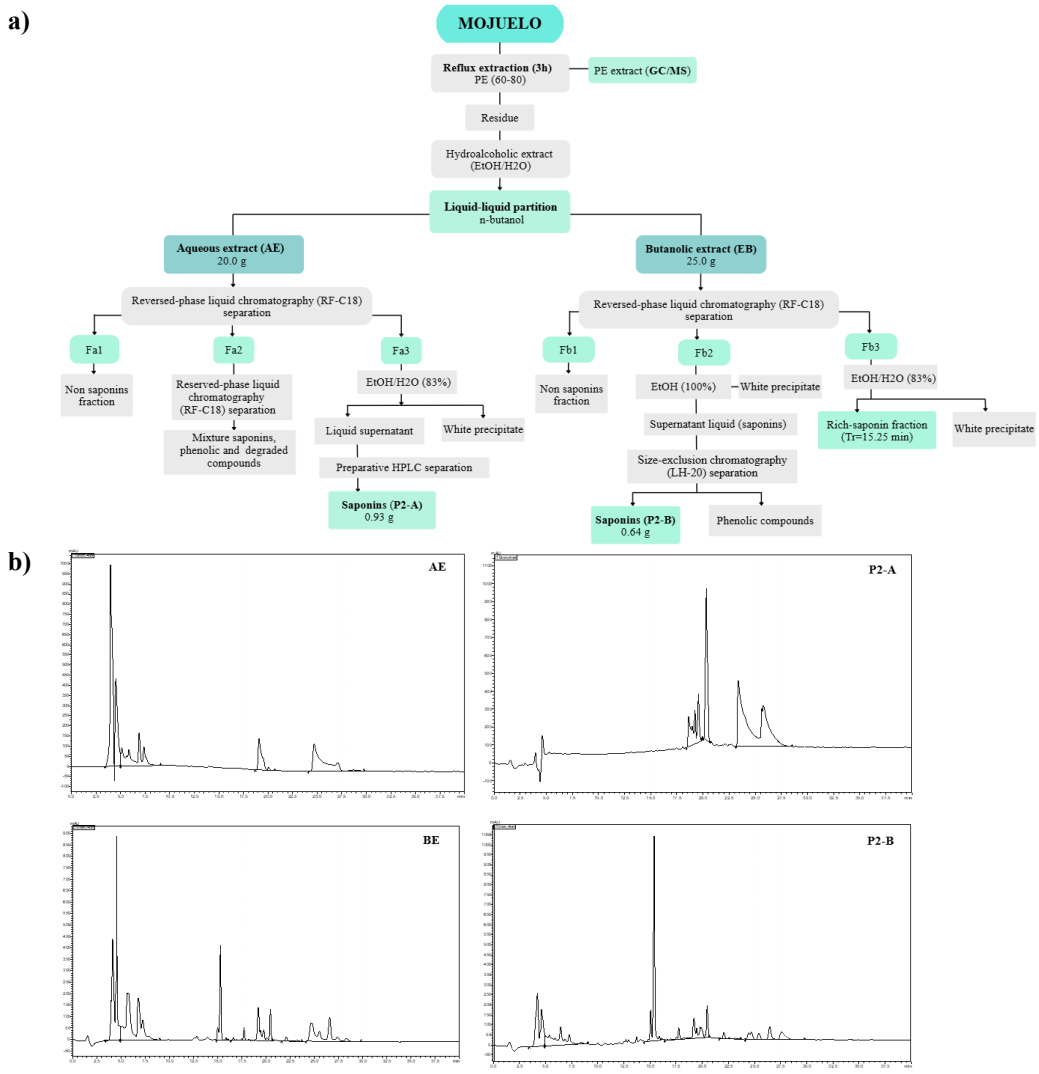

Figure 5. a) Scheme of obtention of saponin-enriched fractions **P2-A** from aqueous extract (**AE**) and **P2-B** from butanolic extract (**BE**), b) HPLC–UV chromatograms of **AE** and **BE** and their corresponding fractions **P2-A** and **P2-B**.

Procedure 3

Finally, **AE** and **BE** were processed using a third procedure, **AE** was subjected to size-exclusion chromatography using Sephadex G-25, while **BE** was treated by ethanol extraction followed by separation on Sephadex LH-20. This process yielded three additional saponin-enriched fractions; **P3-A**, **P3-B1**, and **P3-B2** (Figure 6).

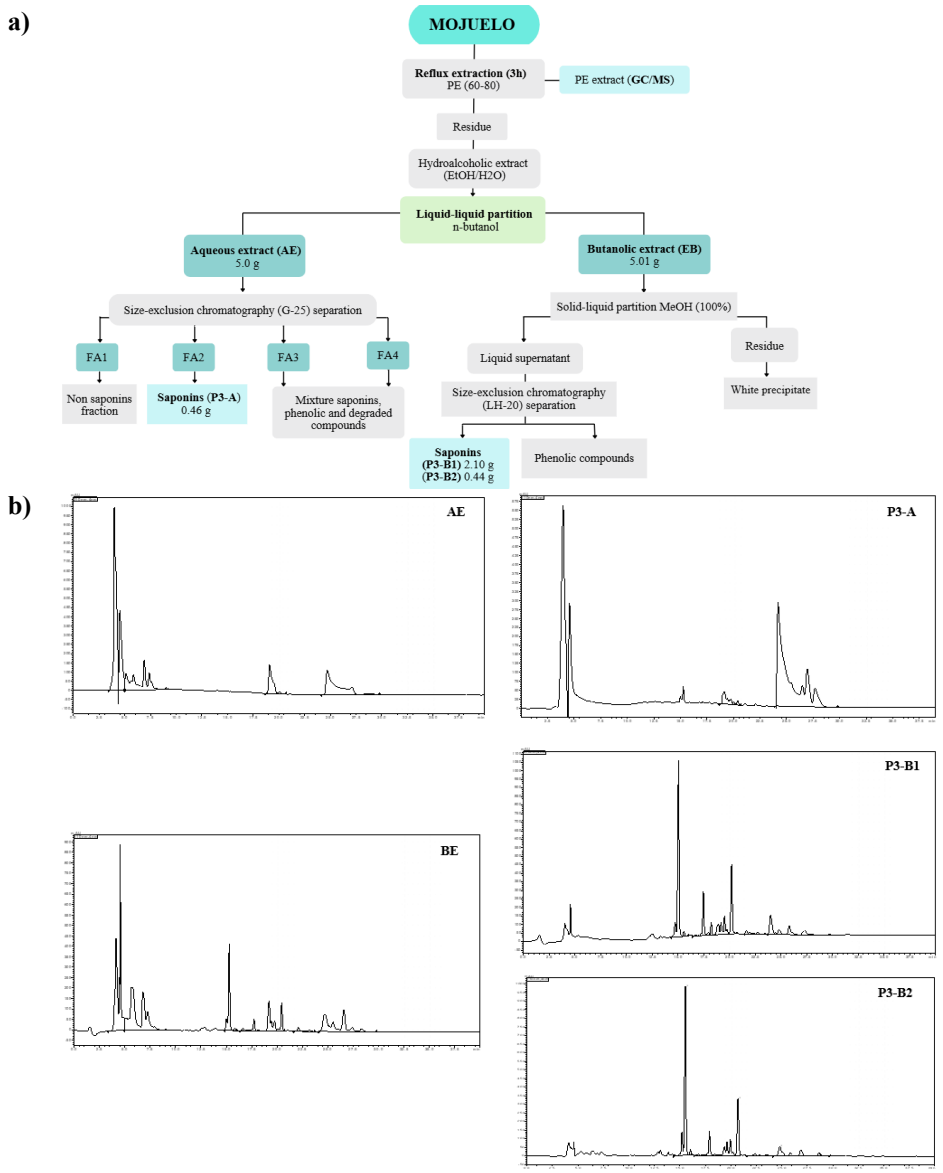

Figure 6. a) Scheme of obtention of saponin-enriched fractions **P3-A** from **AE**, **P3-B1** and **P3-B2** from **BE**, b) HPLC–UV chromatograms of **AE** and **BE** and their corresponding fractions **P3-A**, **P3-B1** and **P3-B2**.

Proposed general protocol for saponin enrichment

Based on the three extraction and fractionation procedures and the LC–ESI–MS chromatographic profiles (Figures 4–6), a general protocol for obtaining saponin-enriched fractions is proposed. First, fatty acids should be removed by extraction with petroleum ether. Subsequently, a hydroalcoholic extraction (H_2O:EtOH, 50:50) should be performed to obtain the crude **HE**. This extract is then subjected to liquid–liquid partitioning with n-butanol.

For the aqueous extract (**AE**), fractionation is carried out using reversed-phase C18 chromatography (RP-C18), followed by further purification using preparative HPLC. In contrast, the butanolic extract (**BE**) is subjected to solid–liquid extraction with ethanol to separate phenolic-rich and saponin-rich fractions. Finally, the saponin-rich fraction is purified by size-exclusion chromatography using Sephadex LH-20.

Quantitative analysis of saponins and phenolic compounds by LC–MS of different saponin-enriched fractions

The quantitative analysis of saponins and phenolic compounds in saponin-enriched fractions was carried out by LC–ESI–MS using the major saponin and phenolic compound previously identified in the hydroalcoholic extract (**HE**) as

external standards. Saponin-**1** (Figure 7) was isolated from the butanolic extract of Quinoa *mojuelo* obtained by liquid–liquid partitioning, followed by successive chromatographic separations. Its structure was elucidated by LC–ESI–MS and NMR spectroscopy. The compound exhibited a retention time (t_R) of 15.25 min and was detected at 210 nm as the most intense peak in the chromatogram.

LC–ESI–MS analysis in positive ion mode revealed a protonated molecular ion at *m/z* 973 $[M+H]^+$, consistent with a bidesmosidic saponin. The fragmentation pattern showed characteristic ions at *m/z* 811 $[M+H–Glc]^+$, 649 $[M+H–Glc–Glc]^+$, and 517 $[M+H–Glc–Glc–Ara]^+$, the latter corresponding to the phytolaccagenic acid (PA) aglycone. This assignment was further supported by the presence of diagnostic fragment ions at *m/z* 499, 481, and 453, which are consistent with typical dehydration and decarboxylation pathways of the triterpenoid core, with *m/z* 481 observed as the base peak. Based on these data, the compound was identified as 3-*O*-*β*-D-glucopyranosyl-(1→3)-*α*-L-arabinopyranosyl-phytolaccagenic acid 28-*O*-*β*-D-glucopyranosyl. The proposed structure was confirmed by comparison of MS and NMR data with previously reported literature[8 15].

Phenolic-**2** (Figure 7) was also isolated from the butanolic extract through liquid–liquid partitioning, followed by size-exclusion chromatography. LC–ESI–MS analysis revealed a retention time of 5.64 min and a protonated molecular ion at *m/z* 741 $[M+H]^+$, consistent with a triglycosylated flavonoid. The fragmentation pattern revealed ions at *m/z* 595 $[M+H–Rha]^+$ (loss of one rhamnose unit, −146 Da), *m/z* 449 $[M+H–Rha–Rha]^+$ (loss of a second rhamnose unit), and *m/z* 287 $[M+H–Rha–Rha–Hex]^+$ (loss of a hexose unit, −162 Da), corresponding to the kaempferol aglycone. This assignment was further supported by the presence of characteristic fragment ions at *m/z* 165, 153, and 137, as well as typical products derived from Retro-Diels–Alder (RDA) cleavage of the C-ring. Overall, these data confirm the presence of a kaempferol triglycoside composed of two rhamnose units and one hexose. Accordingly, Phenolic-**2** was identified as kaempferol-3-*O*-(2,6-di-*O*-*α*-rhamnopyranosyl-*β*-galactopyranoside), commonly known as mauritianin, previously reported as a major phenolic compound in Bolivian quinoa[16].

Saponin-**1** was used as an external standard for the quantification of saponins, whereas kaempferol was used for the quantification of phenolic compounds by LC–ESI–MS. Saponin contents in the analyzed extracts and saponin-enriched fractions were expressed as milligrams of saponin-**1** equivalents per gram of dry extract (mg Sap-1/g), based on the calibration curve ($y=6.66\times10^6x + 1.14\times10^7$, $R^2=0.998$). Phenolic contents were expressed as milligrams of kaempferol equivalents per gram of dry sample (mg KE/g).

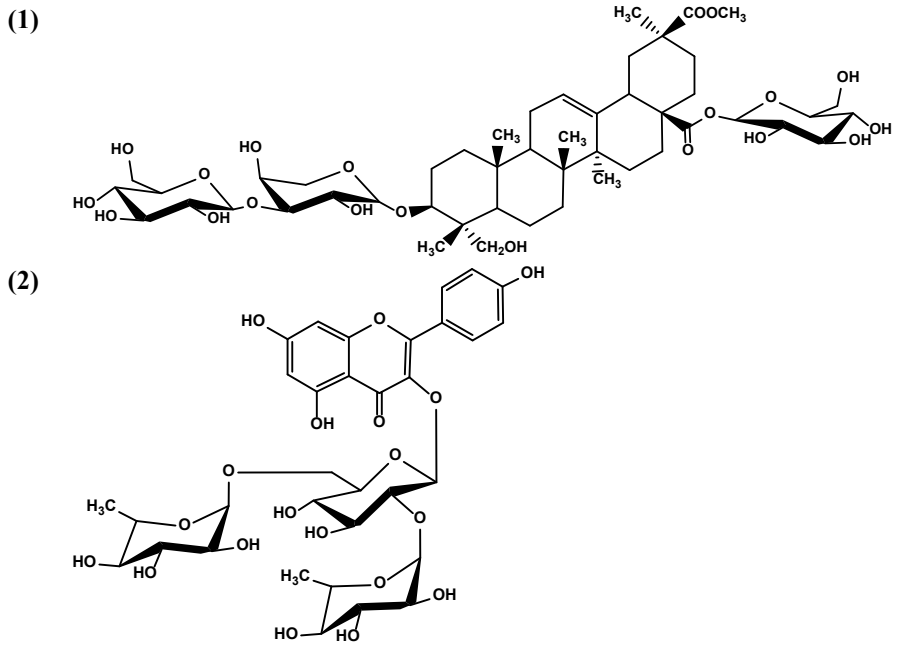

Figure 7. Chemical structures of saponin-**1** and phenolic-**2** used as external standards for quantitative analysis by LC–ESI–MS.

As shown in Table 3, all fractionation procedures (P1–P3) produced fractions with higher saponin content compared to the crude extracts (**HE**, **AE**, and **BE**). Notably, procedures 2 and 3 yielded highly enriched fractions, with saponin contents exceeding 94 % (**P2-A**: 94.7 %, **P2-B**: 95.2 %, **P3-B1**: 97.3 %, and **P3-B2**: 96.0 %), indicating the high efficiency of these purification strategies.
The simultaneous determination of saponins and phenolic compounds (Table 3, Figure 8) further confirms that fractions **P1-B**, **P2-A**, **P2-B**, **P3-B1**, and **P3-B2** are the most enriched in saponins, as highlighted by the dashed circle.

Table 3. Saponin content (mg Sap-1/g and %) and phenolic content (mg KE/g and %) in quinoa extracts and fractions determined by LC-ESI-MS.

Data are expressed as mean ± standard deviation (SD) (n = 3).

Sample	mg KE/g	Phenolic compounds (%)	mg Sap-1/g	Saponins(%)
HE	197 ± 1.0	19.7 ± 0.10	496 ± 9.30	49.6 ± 0.93
BE	294 ± 1.2	29.4 ± 0.12	683 ± 10.6	68.3 ± 1.06
AE	91.4 ± 0.70	9.14 ± 0.07	308 ± 6.53	30.8 ± 0.65
P1-A	44.1 ± 1.0	4.41 ± 0.10	642 ± 10.3	64.2 ± 1.03
P1-B	4.20 ± 1.2	0.42 ± 0.12	903 ± 11.7	90.3 ± 1.17
P2-A	16.8 ± 1.1	1.68 ± 0.11	947 ± 9.52	94.7 ± 0.95
P2-B	8.30 ± 0.9	0.83 ± 0.09	952 ± 8.61	95.2 ± 0.86
P3-A	27.2 ± 0.4	2.72 ± 0.04	464 ± 3.60	46.4 ± 0.36
P3-B1	8.20 ± 0.8	0.82 ± 0.08	973 ± 7.83	97.3 ± 0.78
P3-B2	9.80 ± 0.9	0.98 ± 0.09	960 ± 9.11	96.0 ± 0.91

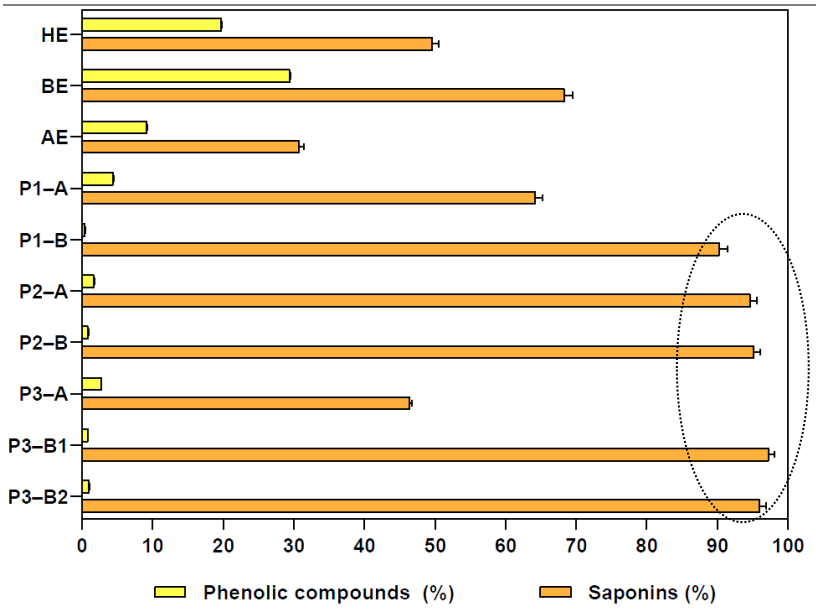

Figure 8. Quantification of saponins and phenolic compounds in the extract and its fractions by LC–ESI–MS.

Spectrophotometric quantification UV–Vis of phenolics and flavonoids
Total flavonoid content was determined by UV–Vis spectrophotometry using quercetin as the reference standard. Quantification was based on the calibration curve (y= 0.0678x+0.0022, R^2 = 0.9986), with absorbance measured at 415 nm. Flavonoid content was expressed as mg of quercetin equivalents (QE) per g of sample.

The hydroalcoholic extract (**HE**) exhibited the highest flavonoid content (0.266 ± 0.013 mg QE/g), followed by the butanolic extract (**BE**) (0.192 ± 0.010 mg QE/g) and the aqueous extract (**AE**) (0.164 ± 0.008 mg QE/g). These results suggest that **HE** represents a suitable matrix for flavonoid extraction due to its intermediate polarity. Saponin-enriched fractions showed significantly lower flavonoid contents, particularly **P1-B** and **P2-B**, indicating efficient separation of

saponins. These findings confirm that fractionation is a key step for the selective isolation of flavonoids with potential biological relevance[17].

Total phenolic content was determined using the Folin–Ciocalteu method, based on the reduction of the Folin reagent by phenolic compounds. Absorbance was measured at 765 nm, and gallic acid was used as the reference standard according to the calibration curve ($y = 0.0081x - 0.0485$, $R^2 = 0.9995$). The results showed significant variations among extracts and fractions (Table 4). The **BE** exhibited the highest phenolic content (13.7 ± 0.24 mg GAE/g), exceeding that of **HE** (5.95 ± 0.20 mg GAE/g) and **AE** (5.93 ± 0.20 mg GAE/g). These findings indicate that phenolic compounds in quinoa *mojuelo* have a higher affinity for moderately polar organic solvents.

All enriched fractions exhibited lower phenolic contents than the crude extracts. However, fractions **P1-A** and **P3-A** retained relatively high phenolic levels, suggesting incomplete separation of phenolic compounds, consistent with the results shown in Figure 8. Overall, solvent extraction and chromatographic fractionation play a critical role in determining the distribution and concentration of phenolic compounds[18].

Table 4. Total phenolic compounds, flavonoid contents, and antioxidant activity (ABTS and DPPH) in extracts and saponin-enriched fractions.

Sample	Flavonoids (mg QE/g)	Total Phenolics (mg GAE/g)	ABTS (% I)	DDPH (% I)	ABTS (µmol TEAC/g)	DPPH (µmol TEAC/g)
HE	0.266 ± 0.013	5.95 ± 0.20	14.88 ± 0.091	3.68 ± 0.084	335 ± 0.26	120 ± 0.12
BE	0.192 ± 0.010	13.7 ± 0.24	19.80 ± 0.072	1.13 ± 0.107	448 ± 0.24	29.1 ± 0.53
AE	0.164 ± 0.008	5.93 ± 0.20	15.12 ± 0.085	3.20 ± 0.197	340 ± 0.81	103 ± 0.12
P1-A	0.127 ± 0.006	4.09 ± 0.15	2.48 ± 0.025	0.97 ± 0.089	49.4 ± 0.39	23.4 ± 0.27
P1-B	0.037 ± 0.002	3.08 ± 0.15	3.71 ± 0.036	1.54 ± 0.133	77.7 ± 0.04	43.7 ± 0.89
P2-A	0.160 ± 0.008	2.18 ± 0.11	2.15 ± 0.109	0.51 ± 0.136	41.8 ± 0.26	7.02 ± 0.03
P2-B	0.030 ± 0.002	2.78 ± 0.14	2.04 ± 0.095	0.73 ± 0.084	39.3 ± 0.13	14.8 ± 0.19
P3-A	0.227 ± 0.016	4.29 ± 0.11	2.43 ± 0.064	0.88 ± 0.277	48.2 ± 0.56	20.2 ± 0.94
P3-B1	0.220 ± 0.011	2.59 ± 0.13	2.39 ± 0.025	0.92 ± 0.089	47.3 ± 0.39	21.6 ± 0.27
P3-B2	0.099 ± 0.005	2.61 ± 0.13	1.23 ± 0.095	0.57 ± 0.197	20.6 ± 0.13	9.16 ± 0.80

All data are expressed as mean ± standard deviation (SD) (n = 3).

Determination of Antioxidant Activity Using ABTS and DPPH Assays

Antioxidant activity was evaluated using ABTS and DPPH radical scavenging assays and expressed both as percentage inhibition (%I) and Trolox equivalents (µmol TEAC/g) (Table 4). The results revealed significant differences between crude extracts (**HE**, **BE**, and **AE**) and saponin-enriched fractions (P1–P3). All crude extracts exhibited higher free radical scavenging capacity than the saponin-enriched fractions. Among them, the butanolic extract (**BE**) showed the highest antioxidant activity in both ABTS and DPPH assays, indicating that antioxidant capacity is strongly associated with phenolic compound content.

This behavior can be attributed to the chemical structure of phenolic compounds, which contain aromatic rings with multiple hydroxyl groups capable of donating electrons or hydrogen atoms and stabilizing free radicals through electron delocalization[19]. This structural feature explains their high reactivity toward $ABTS^{\bullet+}$ and DPPH• radicals *in vitro*. In contrast, saponins lack aromatic systems and generally possess fewer hydroxyl groups involved in redox reactions, which limits their ability to act as efficient radical scavengers[5 6 20 21].

Nevertheless, some saponin-enriched fractions exhibited moderate antioxidant activity. This effect may be attributed to the presence of residual co-extracted phenolic compounds or to structural variations in the saponins, such as differences in the oxidation state of the triterpenoid nucleus.

Additionally, the higher antioxidant activity observed in crude extracts suggests the existence of synergistic interactions between metabolites, which may be partially lost during chromatographic fractionation[5, 18].

In vitro anti-inflammatory activity

Quantification of nitric oxide (NO) production

Macrophage stimulation with lipopolysaccharide (LPS) induces an inflammatory response characterized by the activation of inducible nitric oxide synthase (iNOS) and the subsequent overproduction of nitric oxide (NO). Since excessive NO production is associated with inflammatory processes and tissue damage, its inhibition is widely used as an indicator of the anti-inflammatory activity of natural compounds[22 23]. Treatment with extracts and saponin-enriched fractions (5–15 µg/mL) significantly reduced NO production in LPS-stimulated *RAW 264.7* macrophages (Figure 9),

indicating potential anti-inflammatory activity. Among the crude extracts, the hydroalcoholic (**HE**) and aqueous (**AE**) extracts exhibited moderate inhibition compared with the LPS-stimulated control, suggesting the presence of bioactive metabolites, while (**BE**) butanolic extract showed strong inhibitory effect. Notably, fractions **P1-A**, **P2-A**, and **P3-A** exhibited a more pronounced inhibitory effect, even at lower concentrations, indicating enrichment of active compounds during fractionation[6]. Other fractions, such as **P1-B** and **P3-B1**, showed moderate inhibition, whereas **P2-B** and **P3-B2** displayed variable responses, likely due to differences in chemical composition[6 24]. The observed concentration-dependent decrease suggests that the anti-inflammatory effect may involve inhibition of the LPS-induced pathway, possibly through downregulation of iNOS expression and suppression of NF-κB activation, as widely reported for plant-derived bioactive compounds[25 26].

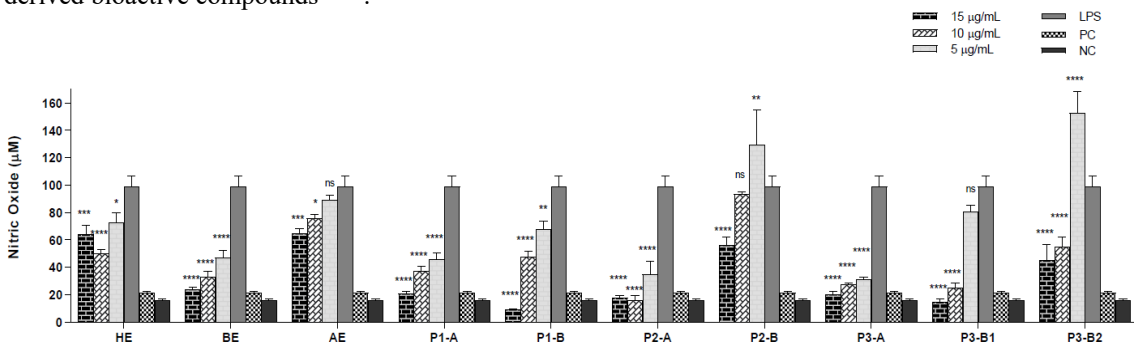

Figure 9. Effect of extracts and saponin-enriched fractions on nitric oxide production in LPS-stimulated *RAW 264.7* macrophages after 24 h of treatment. Nitrite levels were determined by the Griess reaction. Data are expressed as mean ± SE (n = 3). Statistical significance: *p < 0.05, **p < 0.01, *p < 0.001 vs. LPS-treated cells.

Cell viability

Cell viability assessment showed that most extracts and fractions maintained high viability levels in *RAW 264.7* macrophages within the evaluated concentration range (Table 5). The hydroalcoholic (**HE**) and aqueous (**AE**) extracts exhibited a moderate decrease in viability with increasing concentration, with IC_{50} values of 21.7 and 20.6 µg/mL, respectively. In contrast, the butanolic extract (**BE**) showed the highest cytotoxicity, with viability below 70% even at low concentrations and an IC_{50} of 12.9 µg/mL, which may indicate a higher content of bioactive compounds, particularly saponins, known for their cytotoxic effects[21]. Notably, fractions **P1-A**, **P2-A**, **P3-A**, and **P3-B1** exhibited viability values above 100% relative to the control, which may be attributed to inherent variability in colorimetric assays used for cell viability determination[27] or to a potential increase in cellular metabolic activity induced by certain metabolites.

Overall, most fractions presented IC_{50} values higher than 20 µg/mL, indicating a relatively low cytotoxicity profile. These results suggest that the observed inhibition of inflammatory mediators is not primarily associated with cytotoxic effects but rather with a specific modulation of the inflammatory response, which is a key criterion in the evaluation of pharmacologically relevant bioactive compounds[24 26].

Table 5. Cell viability of *RAW 264.7* macrophages treated with extracts and fractions.

Sample	Cell Viability (CV) ± SD(%)			IC50 (µg/ml)
	5 µg/ml	10 µg/ml	15 µg/ml	
HE	97.6 ± 8.32	90.28 ± 4.98	71.0 ± 8.31	21.7
BE	62.8 ± 12.1	52.6 ± 7.95	47.7 ± 10.4	12.9
AE	97.1 ± 6.18	78.9 ± 2.24	67.8 ± 14.8	20.6
P1-A	120.5 ± 14.3	119.1 ± 13.6	112.3 ± 15.1	89.5
P1-B	109.9 ± 12.1	96.7 ± 9.78	82.4 ± 14.6	28.5
P2-A	111.4 ± 22.5	99.6 ± 8.29	69.9 ± 22.6	20.5
P2-B	102.7 ± 4.93	100.0 ± 7.50	78.4 ± 7.50	28.0
P3-A	125.9 ± 11.8	112.8 ± 10.5	88.0 ± 10.5	25.5
P3-B1	138.3 ± 25.3	121.5 ± 7.76	96.4 ± 7.76	26.4
P3-B2	102.9 ± 3.49	99.6 ± 3.13	89.3 ± 3.13	44.6

Inhibition of TNF-α production

The anti-inflammatory activity was further evaluated by measuring the inhibition of tumor necrosis factor-α (TNF-α) production in LPS-stimulated cells (Figure 10). As expected, LPS stimulation significantly increased TNF-α levels compared with the negative control, confirming activation of the inflammatory model, while dexamethasone (positive control) markedly reduced cytokine production.

The **AE** extract showed a strong inhibition of TNF-α production, whereas **HE** and **BE** exhibited moderate, non-significant effects (Figure 10). Fractions **P1-A**, **P2-B**, **P3-A**, and **P3-B1** showed the most pronounced inhibition at both tested concentrations (10 and 15 µg/mL), significantly reducing TNF-α levels compared to LPS-treated cells, indicating a high anti-inflammatory potential. In contrast, **P1-B**, **P2-A**, and **P3-B2** displayed weaker or non-significant effects.
These findings suggest that chromatographic fractionation promoted the enrichment of bioactive compounds responsible for cytokine modulation, likely associated with the increased concentration of saponins, which are known to regulate pro-inflammatory cytokines such as TNF-α [6, 24].

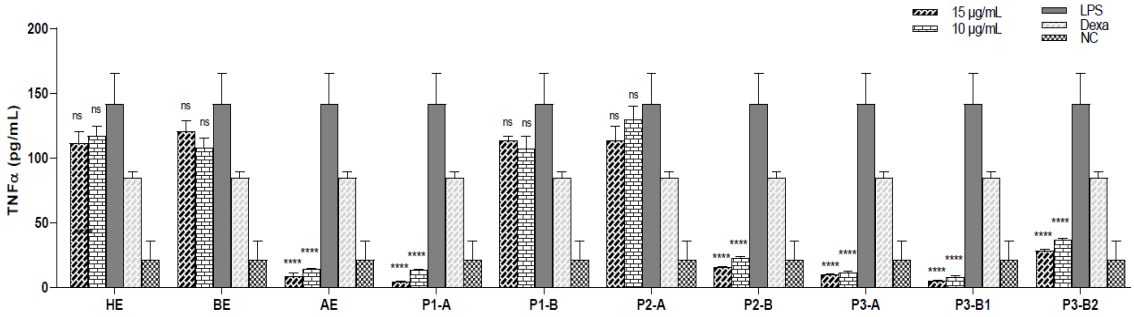

Figure 10. Effect of extracts and saponin-enriched fractions on TNF-α production in LPS-stimulated *RAW 264.7* macrophages. TNF-α levels were determined after 24 h by ELISA. Data are expressed as mean ± SE (n = 3 independent experiments). *p < 0.05, **p < 0.01, ***p < 0.001 vs. LPS.

Inhibition of IL-6 production

The anti-inflammatory activity was further confirmed by evaluating the inhibition of interleukin-6 (IL-6) production in LPS-stimulated cells. LPS treatment significantly increased IL-6 levels compared with the negative control, confirming activation of the inflammatory model[24], while dexamethasone effectively reduced cytokine production.

Among the evaluated samples (Figure 11), fractions **P1-A**, **P1-B**, **P2-A**, **P3-A**, and **P3-B1** exhibited a pronounced inhibitory effect at both tested concentrations (10 and 15 µg/mL), indicating potent anti-inflammatory potential. The **AE** fraction also demonstrated a clear reduction of IL-6 production, while **HE** and **BE** displayed moderate effects. In contrast, **P2-B** and **P3-B2** showed a comparatively lower activity.

These results reinforce the hypothesis that fractionation enhances the concentration of bioactive metabolites, particularly saponins, which may suppress IL-6 production through modulation of key inflammatory signaling pathways[6 24 25 26].

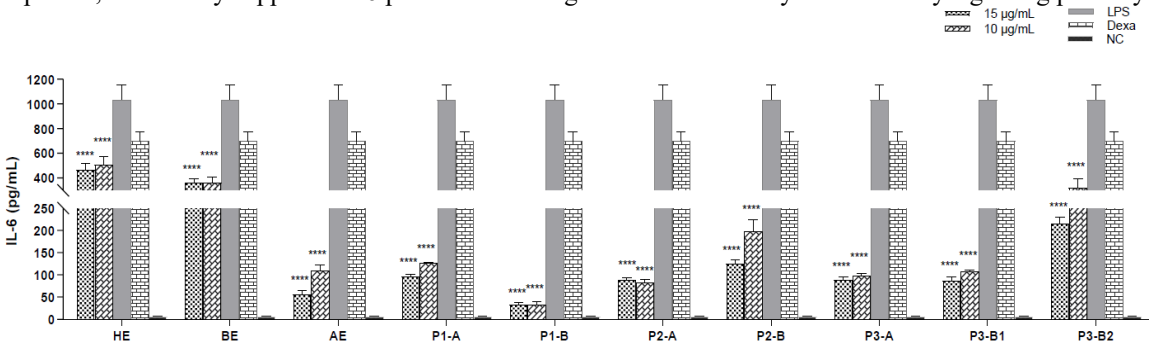

Figure 11. Effect of extracts and saponin-enriched fractions on IL-6 production in LPS-stimulated *RAW 264.7* macrophages. IL-6 levels were determined after 24 h by ELISA. Data are expressed as mean ± SE (n = 3 independent experiments). *p < 0.05, **p < 0.01, ***p < 0.001 vs. LPS.

Modulation of inflammatory mediators (PGE_2 and LTC_4)

LPS stimulation induced a significant increase in PGE_2 levels compared with the negative control, confirming the activation of the *in vitro* inflammatory model. Treatment with extracts and fractions reduced PGE_2 production (Figure 12), with a trend toward greater inhibition at 15 µg/mL. Among crude extracts, **HE** and **AE** showed moderate effects, whereas **BE** exhibited a variable response without consistent inhibitory activity. Notably, fractions **P2-B** and **P3-B2** showed the strongest inhibition at both tested concentrations, while **P1-A** and **P3-B1** reduced PGE_2 levels mainly at 15 µg/mL, suggesting enrichment of active metabolites during fractionation. The inhibition of PGE_2 is particularly relevant since this mediator is produced via cyclooxygenase-2 (COX-2), a key enzyme in inflammation and an important pharmacological target[28 29].

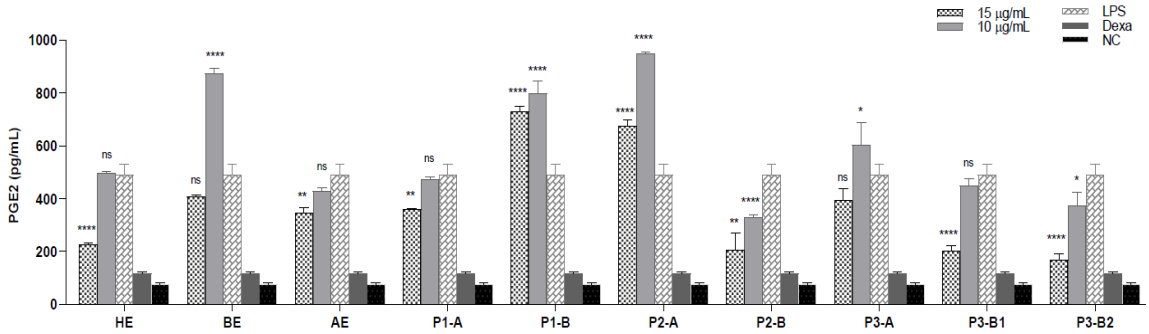

Figure 12. Effect of extracts and enriched fractions on PGE_2 production in LPS-stimulated *RAW 264.7* macrophages. PGE_2 levels were determined after 24 h by ELISA. Data are expressed as mean ± SE (n = 3 independent experiments). *p < 0.05, **p < 0.01, ***p < 0.001 vs. LPS.

Similarly, LPS stimulation increased leukotriene C_4 (LTC_4) levels, whereas treatment with extracts and fractions significantly reduced its production (Figure 13). The enriched fractions displayed a more pronounced inhibitory activity, particularly **P1-A**, **P2-A**, **P2-B**, **P3-A**, **P3-B1** and **P3-B2**, whose LTC_4 levels approached those observed in the negative control or in the positive control treated with dexamethasone. The reduction of LTC_4 is noteworthy, as this mediator is derived from the 5-lipoxygenase (5-LOX) pathway and plays a central role in inflammation, including chemotaxis and vascular permeability[30 31].

Overall, the simultaneous inhibition of PGE_2 and LTC_4 suggests that the bioactive compounds present in these fractions may modulate multiple branches of the arachidonic acid pathway, reinforcing their potential as anti-inflammatory agents.

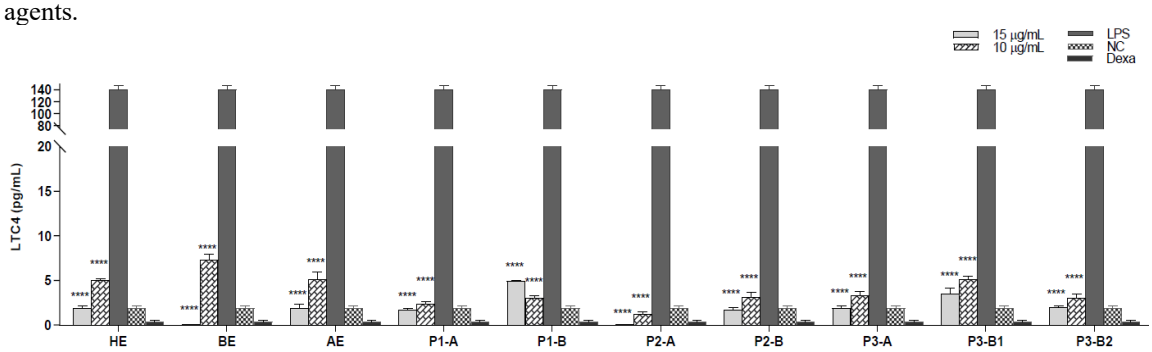

Figure 13. Effect of extracts and enriched fractions on LTC_4 production in LPS-stimulated *RAW 264.7* macrophages. LTC_4 levels were determined after 24 h by ELISA. Data are expressed as mean ± SE (n = 3 independent experiments). *p < 0.05, **p < 0.01, ***p < 0.001 vs. LPS.

EXPERIMENTAL

Materials and methods

Equipment and reagents

All solvents were purchased from Sigma-Aldrich (Merck) and included high-purity acetonitrile (HPLC grade), methanol (HPLC grade), and commercial ethanol (96° GL) obtained from the local market. Methanol, acetonitrile, and n-butanol (analytical grade, p.a.) were used for saponin separation. Most separations were carried out by open-column chromatography and vacuum liquid chromatography (VLC) using silica gel (60 Å pore size) and reversed-phase silica

(RP-C18, 90 Å pore size, 40–63 µm particle size). Thin-layer chromatography (TLC) plates, silica gel 60 F254 (0.50 mm) and RP-C18 F254S (0.25 mm), were purchased from Merck and used for the separation of saponins.
For the identification of each fraction was employed a High-Resolution Liquid Chromatography coupled to mass spectrometer HPLC-MS 2020 series simple quadrupole Shimadzu. Japan combined with SPD-M40 prominence photodiode array detector (DAD). The system was controlled by Lab Solution software and LC-20ADXR Liquid Chromatograph quaternary pump. SIL-40CXR auto sampler CTO-40A prominence column oven. The degassing units DGU-20A3R and DGU-20A5R were used. respectively. The chromatographic saponins separation were done on a Raptor RP (reverse phase) C-18 (254x4.6 mm, 5 µm).

Plant material
All quinoa *mojuelo* samples were obtained from Irupana Andean Food Company (La Paz city. Bolivia) and stored in the bioorganic laboratory at environment conditions.

Saponins extraction
Quinoa *mojuelo* (240 g) were defatted under Soxhlet extraction with petroleum ether $F_{(60\text{-}80)}$ during 3 h then the residue from Soxhlet extraction was extracted with 2 L of aqueous ethanol (1:1, v/v) by stirring during 3 h at 25°C according of procedure described by Lozano, et al, 2012[3] then the hydroalcoholic extract **HE** were dried by rotary-evaporation obtaining 89.0 g of a residue which was dissolved in 400 mL of water and partitioned in four fractions of 100 mL each fraction was subjected to liquid-liquid partitioning with 250 mL of *n*-BuOH by three times and all the *n*-BuOH fractions were joined and dried by rota-evaporation to obtain 33.5 g of butanolic extract **BE**. On the other hand. All the aqueous fractions were joined and dried by lyophilization obtaining 55.0 g of aqueous extract **AE**. The purification of saponins from **AE** and **BE** were done based on three different procedures.

Procedure 1: Saponin enrichment from Aqueous and Butanolic extracts
54.5 g of **AE** were dissolved in 100 mL of water, and proteins were precipitated by isoelectric precipitation at pH 4.3 using 10% (v/v) HCl. The mixture was maintained at 4 °C for 24 h, centrifuged, and the supernatant concentrated to dryness under reduced pressure (52.0 g). A portion (51.5 g) was dissolved in EtOH/H_2O (83:17, *v/v*), yielding a white precipitate (4.05 g) after centrifugation (15 min). The supernatant was concentrated to dryness (48.0 g). A portion (25.0 g) was subjected to RP-C18 column chromatography using a gradient from H_2O/ACN (90:10, v/v) to ACN/MeOH (30:70, v/v), affording four fractions (9.32 g, 6.96 g, 3.79 g and 4.67 g). The ethanol–water precipitate (4.0 g) was further purified by size-exclusion chromatography (Sephadex G-25), yielding a highly polar saponin fraction (**P1-A**, 3.19 g) and a less polar fraction (0.79 g).

Preliminary TLC analyses under normal-phase (NP) and reversed-phase (RP) conditions indicated that BE contained a mixture of saponins and phenolic compounds with similar polarity and apparent molecular weights. Therefore, solid–liquid extraction with ethanol was used as an initial separation step. **BE** (33.2 g) was extracted with ethanol (3 × 1 L), yielding an ethanol-soluble fraction (11.7 g) and an insoluble fraction (21.05 g). The soluble fraction was enriched in phenolic compounds, whereas the insoluble fraction was enriched in saponins. A portion (10.5 g) of the soluble fraction was purified by RP-C18 column chromatography using a gradient from H_2O/ACN (80:20, v/v) to H_2O/ACN (60:40, v/v), followed by ACN/MeOH (30:70, v/v) affording three fractions (2.75 g, 1.69 g and 5.96 g). The first fraction was enriched in glycosylated acids and phenolics, the second mainly contained phenolics, and the third consisted of a mixture of saponins and compounds phenolics. The ethanol-insoluble fraction (20.0 g) was dissolved in EtOH/H_2O (83:17, v/v), yielding a white precipitate (4.30 g) after decantation and centrifugation (25 min). The supernatant was concentrated under reduced pressure (15.6 g), and a portion (15.0 g) was subjected to size-exclusion chromatography on Sephadex G-25, affording a saponin-rich fraction (**P1-B**, 8.89 g) and a phenolic-rich fraction (5.76 g).

Procedure 2: Saponin enrichment from Aqueous and Butanolic extracts
AE (20.0 g) was subjected to RP-C18 chromatography using a gradient of 85–50% H_2O/ACN followed by 45–60% ACN/MeOH, yielding three fractions (0.09 g, 14.8 g and 5.08 g). A portion (10.0 g) of the second fraction was further purified by RP-C18 chromatography using a gradient from H_2O/ACN (80:20, v/v) to H_2O/ACN (50:50, v/v), followed by ACN/MeOH (45:55, v/v), affording four fractions (0.59 g, 0.76 g, 6.28 g and 2.41 g). The third fraction (4.50 g) was resuspended in EtOH/H_2O (83:17, v/v), yielding a white precipitate (0.96 g). After decantation and centrifugation (25 min), the supernatant yielded 3.54 g. A portion (3.50 g) was purified by preparative HPLC. The system consisted of a Shimadzu instrument equipped with a Restek Ultra C-18 column (5 µm, 100 × 10 mm), a UV–Vis detector (SPD-20A), an isocratic pump (LC-20AP), and a fraction collector. The method was based on Lozano et al. (2012). Isocratic elution was performed using 15% (*v/v*) acetonitrile and 0.1% formic acid at a flow rate of 1 mL/min. The sample was filtered

through a 0.45 µm membrane, and 500 µL were injected and monitored at 210 nm. Fractions (~3 mL) were collected. A broad peak at 12.2–15.5 min yielded 1.98 g of compound **P2-A**.
BE (25.0 g) was subjected to RP-C18 chromatography using a gradient of 80–50% H_2O/ACN followed by 45–50% ACN/MeOH, yielding three fractions (0.59 g, 13.1 g and 11.3 g). A portion (12.0 g) of the second fraction was purified by size-exclusion chromatography on Sephadex LH-20 using 100% EtOH, yielding a white precipitate (4.86 g) and a supernatant (7.14 g). The supernatant was further separated on LH-20, affording five fractions; **P2-B** (0.64 g) and additional fractions (3.12 g, 0.47 g, 0.16 g and 2.62 g). The third fraction (10.0 g) was resuspended in EtOH/H_2O (83:17, *v/v*), yielding a white precipitate. After decantation and centrifugation (25 min), the precipitate weighed 0.79 g and the supernatant 9.21 g. Finally, a portion (9.02 g) of the supernatant was purified by size-exclusion chromatography on Sephadex G-25 using 100% H_2O as isocratic elution, yielding three fractions (5.69 g, 1.07 g and 2.25 g).

Procedure 3: Saponin enrichment from Aqueous and Butanolic extracts
5.0 g of **AE** was subjected to size-exclusion chromatography on a Sephadex G-25 column, using an isocratic elution system with 100% H_2O as the mobile phase. Four fractions were obtained, with yields of 0.35 g, 0.46 g (**P3-A**), 1.02 g and 3.15 g, respectively.

Additionally, 5.01 g of **BE** was subjected to chromatographic separation using an isocratic elution system with 100% MeOH. After dissolution of the sample, the formation of a white precipitate was observed, which was recovered by physical separation, yielding 1.23 g and corresponding to the ethanol-insoluble fraction. The supernatant constituted the ethanol-soluble fraction (3.75 g). Subsequently, 3.61 g of this soluble fraction was further fractionated by size-exclusion chromatography on an LH-20 column, yielding seven fractions with yields of 2.10 g (**P3-B1**), 0.44 g (**P3-B2**), 0.41 g, 0.32 g, 0.26 g, 0.03 g and 0.05 g respectively.

Saponins and phenolic analysis by LC-MS
Saponin-**1** and Phenolic-**2** were isolated from the butanolic extract (**BE**). The extract was subjected to reverse-phase vacuum liquid chromatography (VLC) on a C18-packed column using a water–methanol gradient (40:60 to 20:80, *v/v*), yielding several fractions, from which Saponin-**1** was obtained. Fractionation was monitored by thin-layer chromatography (TLC) on normal-phase (NF) and reversed-phase[32] plates. One of the fractions obtained from the VLC separation was subsequently repurified by size-exclusion chromatography on a Sephadex G-25 column using water as the isocratic eluent, leading to the isolation of Phenolic-**2**. The purity of the isolated compounds was finally assessed by LC–MS analysis.

Analyses were performed using LC–ESI–MS, with 10 µL of sample solutions (10 mg/mL) injected. The mobile phase consisted of 0.1% formic acid in water (A) and acetonitrile (B), delivered at a flow rate of 0.5 mL/min. A linear gradient was applied, decreasing from 75% to 65% A over 15 min, followed by a further decrease from 65% to 55% A. The ESI source operated in negative-ion mode (capillary voltage 4 kV), with nitrogen as the drying gas at 13 L/min and 350 °C, and a scan range of m/z 200–1400. This method was used for the quantification of saponins and the semi-quantification of phenolic compounds.

For saponin quantification, a calibration curve was constructed using a previously isolated and characterized saponin as the reference standard, confirmed by NMR spectroscopy and LC–ESI–MS (tR = 15.25 min). A stock solution (25 mg/mL) was prepared by dissolving 50 mg of the standard in 2 mL of an acetonitrile–water mixture (60:40, v/v). Working standard solutions (10–22 mg/mL) were analyzed under the same chromatographic conditions, and calibration curves were constructed by plotting peak area versus concentration. Analyses were performed in triplicate, and only calibration curves with a correlation coefficient ($R^2 \geq 0.99$) were accepted.

Phenolic compounds were semi-quantified using a single-point external standard approach due to their low abundance and the limited availability of a reference standard. A kaempferol standard solution (10 mg/mL), prepared by dissolving 5 mg in 500 µL of solvent, was used, and its chromatographic peak area served as a reference to estimate phenolic compounds in the extracts and enriched fractions. Kaempferol showed a retention time (T_R) of 5.64 min under the applied chromatographic conditions. The peak area of the standard was higher than that of the samples, ensuring adequate sensitivity within the working range. Semi-quantification was performed in triplicate based on relative response, assuming similar detector response factors for structurally related compounds.

Quantification of phenolic compounds and flavonoids
Determination of Total Flavonoids
The total flavonoid content was determined using a colorimetric method based on the formation of the flavonoid–$AlCl_3$ complex. The samples were analyzed by UV–Vis spectrophotometry at 406 nm after reaction with ethanol, aluminum

chloride 10% (*v/v*) and potassium acetate 1 M followed by incubation for 30 min at room temperature. The quantification was performed using a calibration curve constructed with quercetin in the range of 2–12 ppm. and results were expressed as milligrams of quercetin equivalents per gram of sample (mg QE/g). All determinations were performed in triplicate and reported as mean ± standard deviation. Analyses were conducted at a final concentration of 80 ppm for ~~the~~ extracts and 40 ppm for fractions.

Determination of Total Phenolic Content

Total phenolic content was determined using the Folin–Ciocalteu colorimetric method. with slight modifications to the procedures described by Dogan, et al, 2021[33 34]. The reaction was carried out following the sequential addition of the Folin–Ciocalteu reagent previously diluted (1:10 *v/v*) and sodium carbonate solution 7.5% (*w/v*) followed by incubation for 30 min at 40 °C. Absorbance was recorded at 765 nm and the quantification was performed using a calibration curve prepared with gallic acid over the concentration range of 10–70 mg/L. The results were expressed as milligrams of gallic acid equivalents per gram of sample (mg GAE/g). All determinations were performed in triplicate and the data were reported as mean ± standard deviation with samples analyzed at final concentrations of 15 ppm for extracts and 10 ppm for fractions.

Inorganic characterization

To complement matrix characterization, the inorganic fraction was analyzed using X-ray–based techniques. X-ray diffraction (XRD) was performed using a diffractometer from Rigaku model MiniFlex, equipped with a Cu Kα radiation source (λ = 1.54 Å). The sample was finely ground using a mortar and placed in an aluminum sample holder. Diffractograms were recorded at a scanning rate of 10°/min with a step size of 0.01°, and the data were acquired and processed using SmartLab Studio.

Elemental analysis was carried out by energy-dispersive X-ray fluorescence (EDS-XRF) using a spectrometer from Rigaku model EDS-XRF QuantEZ QC+. The sample was finely ground to obtain a homogeneous powder, placed in a polypropylene sample holder (≈75 % capacity), and manually pressed (~79 N, 1 min) using a protective film of the same material. Measurements were performed under conditions optimized for light elements (6.5 kV, 156 µA, 30 s), using Kα spectral lines. Data acquisition and processing were carried out using the instrument's integrated software (NEX).

Determination of antioxidant activity using ABTS and DPPH assays

The antioxidant activity of the samples was evaluated using the $ABTS^{\bullet+}$ cation radical inhibition and DPPH free radical scavenging assays following methodologies previously reported by Prior, et al 2005[34 35 36]. The $ABTS^{\bullet+}$ radical was generated from the reaction between ABTS (7 mM) and potassium persulfate (2.45 mM) and the solution was kept in the dark at room temperature for 12–16 h. Prior to analysis. This solution was diluted with ethanol to reach an absorbance of 0.700 ± 0.02 at 734 nm. Antioxidant activity was determined by UV–Vis spectrophotometry at 734 nm after the reaction of the samples with the radical solution. and results were expressed as micromoles of The Trolox-equivalent antioxidant capacity (TEAC) per gram of sample (µmol TE/g) using a calibration curve prepared with Trolox in the range of 10–100 µM.

The DPPH assay was performed using a methanolic DPPH solution (60 µM). and the decrease of absorbance was recorded at 515 nm after incubating the samples in the dark for 30 min. Quantification was carried out using a Trolox standard curve in the range of 100–800 µM. and results were expressed as the Trolox-equivalent antioxidant capacity (TEAC) per gram of sample (µmol TE/g). All analyses were performed in triplicate and data were reported as mean ± standard deviation. Samples were evaluated at final concentrations of 10 ppm for extracts and fractions in both the ABTS and DPPH assays.

In vitro anti-inflammatory activity

Cell culture

The murine macrophage cell line *RAW 264.7* was recovered from cryopreservation and cultured in Roswell Park Memorial Institute (RPMI) medium supplemented with 10% heat-inactivated fetal bovine serum (FBS), penicillin (100 U/mL), and streptomycin (100 µg/mL). Cells were maintained at 37 °C in a humidified incubator with 5% CO_2. For experimental assays, adherent cells were gently detached by pipetting, centrifuged at 1500 rpm for 5 min, and resuspended in RPMI medium supplemented with 10% FBS for cell counting and viability assessment. Cells were seeded in 24-well plates at a density of 1×10^5 cells/mL and allowed to adhere for 12 h prior to treatment.

Quantification of nitric oxide and pro-inflammatory cytokines (IL-6 and TNF-α) in LPS-stimulated cells

After the adhesion period, the culture medium was replaced with fresh RPMI medium containing 10% FBS and the extracts or saponin-rich fractions at concentrations of 10 and 15 µg/mL. Inflammatory stimulation was induced by the addition of lipopolysaccharide (LPS) from *Escherichia coli* with the concentration of 1 µg/mL[22, 23]. Dexamethasone (1 µg/mL) was used as positive control. Following 24 h of incubation, culture supernatants were collected and stored at −80 °C until analysis. Nitric oxide production was evaluated by measuring nitrite levels in each assay, a stable end product of NO metabolism, using the Griess reaction as previously described[37]. Absorbance was measured at 550 nm, and nitrite concentrations were calculated from a sodium nitrite ($NaNO_2$) standard curve prepared in culture medium. The levels of the pro-inflammatory cytokines interleukin-6 (IL-6) and tumor necrosis factor-α (TNF-α) were quantified using commercially available ELISA kits (BD Biosciences), following the manufacturer's instructions.

Evaluation of cytotoxicity

The cytotoxic effects of the extracts and saponin-enriched fractions were evaluated in *RAW 264.7* cells treated with concentrations of 10 and 15 µg/mL for 24 h. Cell viability was assessed using the MTT colorimetric assay. Briefly, the culture medium was removed and replaced with 100 µL of MTT solution (1 mg/mL) prepared in phenol red–free RPMI medium, followed by incubation for 4 h at 37 °C. The resulting crystals were solubilized with 150 µL of 0.04 N isopropanol–HCl, and absorbance was measured at 550 nm using 620 nm as the reference wavelength. Cell viability was expressed as a percentage relative to untreated control cells[27].

Statistical analysis

All experiments were performed in triplicate, and the results are expressed as mean ± standard error (SE). Statistical analyses were carried out using GraphPad Prism 8 (GraphPad Software, San Diego, CA, USA). Comparisons among multiple groups were performed using one-way analysis of variance (ANOVA) followed by Tukey's post hoc test. In experiments involving two independent variables, two-way ANOVA was applied when appropriate. Differences between groups were considered statistically significant at $p < 0.05$.

CONCLUSIONS

This study established reproducible and efficient fractionation protocols to derive high-purity saponin-enriched fractions (>94%) from quinoa scarification by-products (*mojuelo*). The systematic integration of liquid–liquid partitioning with orthogonal chromatographic techniques allowed for the effective separation of complex triterpenoid saponins from the phenolic-rich matrix.

Biological evaluation revealed that these saponin-enriched fractions possess potent anti-inflammatory activity, evidenced by the significant suppression of pro-inflammatory mediators (NO, TNF-α, IL-6) and the dual modulation of the COX-2 and 5-LOX pathways via the reduction of PGE2 and LTC4 levels. Conversely, the antioxidant capacity was found to be primarily localized within the crude phenolic-rich extracts, suggesting that the valorization of *mojuelo* should be tailored toward the specific bioactivity of interest.

Overall, these findings demonstrate that quinoa industrial residues represent a high-value reservoir of bioactive secondary metabolites. The proposed methodologies facilitate the standardization of quinoa-derived products, providing a sustainable biochemical rationale for their integration into advanced nutraceutical and pharmaceutical formulations.

ACKNOWLEDGEMENTS

The authors gratefully acknowledge Irupana Andean Organic Food company for supplying scarified quinoa "*mojuelo*". We also gratefully acknowledge financial support from the Swedish International Development Cooperation Agency through Subprogram 6 "Bio-inputs from Agro-industrial Waste" and Subprogram 17 "Biomolecules of Medicinal and Industrial Interest", as well as from the SATREPS project "Strengthening of resilience in arid agro-ecosystems vulnerable to climate change, through research on plant resources and technological applications" (SATREPS; Grant No. JPMJSA1907). These subprograms and project provided the equipment, reagents, and materials, as well as financial support for Carolina Triguero's MSc thesis.

REFERENCES

[1] S. Zwenger, C. Basu, *Biotechnol. Mol. Biol. Rev.*, 2008 **3**, 1. DOI: 10.5897/BMBR2023.0292

[2] R. F. A. Casalvara, B. M. R., Ferreira, J. E., Gonçalves, N. U., Yamaguchi, A. Bracht, L. Bracht, J. F.Comar, A. B. de Sá-Nakanishi, C. G. M. de Souza, R. Castoldi, *Nutrients*, 2024 **16**, 840. DOI: 10.3390/nu16060840

[3] M. Lozano, E.Tícona, C.Carrasco, Y. Flores, G. R. Almanza, *Rev. boliv. quim.*, 2012 **29**, 131.
[4] T. Kuljanabhagavad, P. Thongphasuk, W. Chamulitrat, M. Wink., *Phytochem.*, 2008 **69**, 1919. DOI: 10.1016/j.phytochem.2008.03.001
[5] Francis, G.; Kerem, Z.; Makkar, H. P.; Becker, K., *British journal of Nutrition*, 2002 **88**, 587.
[6] S. Sparg, M. Light, J. Van Staden, *J. ethnopharmacol.*, 2004 **94**, 219. DOI:10.1016/j.jep.2004.05.016
[7] R. Villagomez, M.; Lozano, Y. R. Flores, Y. Kobayashi, , Y. Fujita, G. R., Almanza, *ACS omega*, 2025 **11**, 46. DOI: org/10.1021/acsomega.5c01812
[8] T. Mad, H. Sterk, M. Mittelbach, G. N Rechberger, *J. Am. Soc. Mass Spectrom*, 2006 17, 795. DOI: 10.1016/j.jasms.2006.02.013
[9] A. M. Gómez-Caravaca, G. Iafelice, A. Lavini, C. Pulvento, M. F. Caboni, E. Marconi, *J Agric. Food Chem*, 2012 **60**, 4620. DOI: 10.1021/jf3002125
[10] R. Przybylski, G. Chauhan, N. Eskin, *Food Chem.*1994 **51**, 187. DOI:10.1016/0308146(94)902550
[11] A. Vega-Gálvez, M. Miranda, J. Vergara, , E. Uribe, L. Puente, E. A. Martínez, *Journal of the Science of Food and Agriculture*, 2010 **90**, 2541. DOI: 10.1002/jsfa.13753
[12] Y.Tang, X. Li, B. Zhang, P. X. Chen, R. Liu, R.Tsao, *Food chem.*, 2015 **166**, 380 DOI: 10.1016/j.foodchem.2014.06.018
[13] C. Fanali, M. Beccaria, S. Salivo, P. Tranchida, G. Tripodo, S. Farnetti, L. Dugo, P. Dugo, L.Mondello, *J. Sep. Sci.*, 2015 **38**, 3151. DOI: 10.1002/jssc.201500466
[14] G. N. Carpio-Paucar, A. I. Palo-Cardenas, A. N. Rondón-Ortiz, A. Pino-Figueroa, E. G. Gonzales Condori, J. A. Villanueva-Salas, *J. Scientific.,* **2023**, 8846387. DOI: 10.1155/2023/8846387
[15] G. M. Woldemichael, M. Wink, *J. Agric. Food Chem.*, 2001 **49**, 2327. DOI: 10.1021/jf0013499
[16] A. Navia, P. Ormachea, L. Salcedo, M. Lozano, S. Tarqui, Y. Flores, G. R. Almanza, *Rev. bol quím*, 2020 **37**, 12.
[17] A. N. Panche, A. D. Diwan, S. R. Chandra, *J. Nutr. Sci.*, 2016 **5**, e47. DOI: 10.1017/jns.2016.41
[18] F. Shahidi, P. Ambigaipalan, *J. Funct. Foods.*, 2015 **18**, 820. DOI: 10.1016/j.jff.2015.06.018
[19] J. Dai, R. J. Mumper, *Molec.*, 2010 **15**, 7313. DOI: 10.3390/molecules15107313
[20] I. Podolak, A. Galanty, D. Sobolewska, *Phytochem. Rev.,* 2010 **9**, 425. DOI: 10.1007/s111010109183z
[21] S. Man, W. Gao, Y. Zhang, L. Huang, C. Liu, *Fitoterapia*, 2010 **81**, 703.DOI: 10.1016/j.fitote.2010.06.004
[22] F. Aktan, *Life sci.*, 2004 **75**, 639. DOI: 10.1016/j.lfs.2003.10.042
[23] S. Moncada, R. Palmer, E. Higgs, *Pharma. Rev.*, 1991 **43**, 109. DOI 10.1016/S0031-6997(25)066633
[24] J. B. Calixto, M. M. Campos, M. F. Otuki, A. R. Santos, *Planta medica*, 2004 **70**, 93. DOI: 10.1055/s-2004-815483
[25] T. Lawrence. *Cold Spring Harb. Perspect. Biol*., 2009 **1**, a001651. DOI: 10.1101/cshperspect.a001651
[26] S. Reuter, S. C. M. M. Gupta, B. B., Chaturvedi, Aggarwal, *Free Radic. Biol. Med.*, 2010 **49**, 1603. DOI: 10.1016/j.freeradbiomed.2010.09.006
[27] T. Mosmann, *J. Immunol. Methods*, 1983 **65**, 55. DOI: 10.1016/0022-1759(83)90303-4
[28] E. Ricciotti, G. A. FitzGerald, *Arterioscler. Thromb. Vasc. Biol.***,** 2011 **31**, 986. DOI: 10.1161/ATVBAHA.110.207449
[29] J. Y. Park, M. H. Pillinger, S. B. Abramson, *Clin. Immunol*, 2006 **119**, 229. DOI: 10.1016/j.clim.2006.01.016
[30] M. Peters-Golden, W. R., Henderson Jr, *N Engl J Med.,* 2007 **357**, 1841. DOI: 10.1056/NEJMra071371
[31] O. Rådmark, O. Werz, D. Steinhilber, B., Samuelsson, *Trends Biochem. Sci.* 2007 **32**, 332. DOI: 10.1016/j.tibs.2007.06.002
[32] W.; Oleszek, A. Hamed,. *J. of Surfactants and Detergents*, 2010, 239. DOI: 10.1002/jsde.12216
[33] N. Doğan, C. Doğan, *Trak. Univ. J. Nat. Sci.*, 2021. DOI:10.23902/trkjnat.960073
[34] R. L. Prior, X. Wu, K. Schaich, *J. Agric. Food Chem.*, 2005 **53**, 4290. DOI: 10.1021/jf0502698
[35] S. Fakoya, K. Adegbehingbe, I. Ademakinwa, S. Fakoya, K. Adegbehingbe, I. Ademakinwa, *Open J. Med. Microbiol.*, 2020 **10**, 58. DOI: 10.4236/ojmm.2020.102006
[36] G. Sudha, S. Vadivukkarasi, R. B. I. Shree, P. Lakshmanan, *Food Sci. Biotechnol*, 2012 **21**, 661.
[37] L. C. Green, D. A. Wagner, J. Glogowski, P. L. Skipper, J. S. Wishnok, S. R. Tannenbaum, *Anal. Biochem.,* 1982 **126**, 131. DOI: 10.1016/0003-2697(82)90118-X